phys. stat. sol. (c) **3**, No. 11, 3827–3831 (2006) / **DOI** 10.1002/pssc.200671551

Microscopic tight-binding description for electronic and optical properties of InN/GaN quantum dots

S. Schulz[*1], **N. Baer**[1], **S. Schumacher**[1,2], **P. Gartner**[1,3], **F. Jahnke**[1], and **G. Czycholl**[1]

[1] Institute for Theoretical Physics, University of Bremen, P.O. Box 330440, 28334 Bremen, Germany
[2] Currently at: College of Optical Sciences, University of Arizona, Arizona, Tucson 85721, USA
[3] Institute for Materials Physics, P.O. Box MG-7, Bucharest-Magurele, Romania

Received 1 May 2006, revised 14 June 2006, accepted 18 July 2006
Published online 24 November 2006

PACS 71.35.–y, 73.21.La, 73.22.Dj, 78.55.Cr, 78.67.Hc

Electronic and optical properties of self-assembled InN/GaN quantum dots are investigated by use of a tight-binding model combined with a configuration interaction calculation. Dipole and Coulomb matrix elements are calculated from the single-particle wavefunctions which fully include the atomistic wurtzite structure of the low-dimensional heterostructure and serve as input parameters for the calculation of optical properties. We discuss in particular the influence of the internal electric field on the multi-exciton spectra. Dark exciton and biexciton ground-states are found for small quantum dots.

1 Introduction

Semiconductor quantum dots (QDs) are subject of intense experimental and theoretical research. As a new material system, group-III nitrides are of particular interest due to their wide range of emission frequencies from amber to ultraviolet. In the following, we study self-assembled InN/GaN QDs in the wurtzite phase. The one-particle states are calculated by means of a tight-binding (TB) model, which provides a powerful approach to the electronic states of low-dimensional heterostructures on an atomistic level [1, 2]. For the calculation of optical absorption and emission spectra, configuration-interaction (CI) calculations [3, 4] are used to obtain a consistent description of correlated many-particle states. The calculation of dipole and Coulomb matrix elements from the TB one-particle wave functions [5, 6] allows to combine these two approaches and facilitates the investigation of optical transitions between the interacting many-particle states of QDs with parameters obtained from a microscopic model.

2 Theory

To reproduce the characteristic properties of the bulk band structures of wurtzite InN and GaN in the vicinity of the Γ point, we use a TB-Model with an sp^3-basis $|\nu, \alpha, \boldsymbol{R}\rangle$. More precisely, we use one s-state ($\alpha = s$) and three p-states ($\alpha = p_x, p_y, p_z$) per spin direction at each site ν inside the unit cell $\boldsymbol{R}$. Non-diagonal TB-matrix elements are included up to nearest neighbors. The small spin-orbit coupling and crystal-field splitting are neglected. Therefore, by using the two center approximation of Slater and Koster [7], we are left with nine independent matrix elements. These matrix elements are empirically determined by fitting the TB band structure to band structure calculations and available experimental data [8, 9] so that the characteristic properties of the band structure around the Γ point are well reproduced.

* Corresponding author: e-mail: sschulz@itp.uni-bremen.de, Phone: +49-421-218 2965, Fax: +49-421-218 4869

Starting from the bulk TB-parameters, the QD is modeled on an atomistic level, such that for each site the matrix elements are set according to the occupying atoms. For the nitrogen (N) atoms at the interface between GaN and InN we use an averaged value for the on-site matrix elements. The valence band offset ΔE_v between the two materials (InN and GaN) is included in our model by shifting the diagonal matrix elements of the bulk InN. We assume here a valence-band offset between the two materials of $\Delta E_v = 0.5$ eV [10]. To model an InN QD embedded in a GaN barrier material, a cell with fixed boundary conditions is chosen. A sufficiently large supercell is required to avoid numerical artefacts in the localized QD states due to the cubic symmetry of the boundaries. Inside this box we consider an InN wetting layer (WL) with a thickness of one lattice constant in z-direction of the conventional unit cell, and on top of this a lens-shaped InN QD. As a first approximation we neglect the lattice mismatch between InN and GaN. Since we are interested in more general aspects to bridge the gap between the single-particle properties and the many-body problem, we neglected the strain induced displacements of the atoms. In case of, for example, elongated pyramidal QD structures strain could be important and may affect the ordering of the single particle states. For the chosen QD geometry, however, the more realistic inclusion of strain effects does not change the symmetry so that the general statements should also hold if strain effects were included in our calculation. Surface effects, stemming from the fixed boundary conditions of the finite supercell, are avoided by the method described in Ref. [11]. The spontaneous polarization in the wurtzite crystal structure and the strong strain-induced piezoelectric field are included according to Ref. [12].In case of InN and GaN several different values for material parameters have been reported in the literature. These variations are mainly caused by the fact that it is difficult to grow sufficiently large bulk crystals [13]. Nevertheless, even with different values for the material parameters a similar qualitative behavior for the ordering of the single-particle states can be expected. Different values for material parameters would mainly yield an overall shift of the single-particle energy spectrum. A discussion and an overview of the influence of different elastic and piezoelectric constants on the built-in field is given in Ref. [14]. The TB-Hamiltonian of the whole cell corresponds to a finite but huge matrix. Therefore, the eigenstates and eigenenergies must be determined by efficient matrix diagonalization algorithms. For this purpose we employ the folded spectrum method (FSM) [15] combined with parpack routines.

For the calculation of optical spectra, Coulomb and dipole matrix elements between the TB single-particle wavefunctions are required. As the atomic orbitals are not explicitly known in an empirical TB approach, we approximate the Coulomb matrixelements by:

$$V_{ijkl} = \sum_{\mathbf{R}\mathbf{R}'} \sum_{\alpha\beta} c^{i*}_{\mathbf{R}\alpha} c^{j*}_{\mathbf{R}'\beta} c^{k}_{\mathbf{R}'\beta} c^{l}_{\mathbf{R}\alpha} V(\mathbf{R}-\mathbf{R}')\,, \tag{1}$$

$$\text{with} \quad V(\mathbf{R}-\mathbf{R}') = \frac{e_0^2}{4\pi\varepsilon_0\varepsilon_r|\mathbf{R}-\mathbf{R}'|} \quad \text{for} \quad \mathbf{R}\neq\mathbf{R}'$$

$$\text{and} \quad V(0) = \frac{1}{V_{uc}^2}\int_{uc} d^3r\, d^3r' \frac{e_0^2}{4\pi\varepsilon_0\varepsilon_r|\mathbf{r}-\mathbf{r}'|} \approx V_0\,. \tag{2}$$

The $c^i_{\mathbf{R},\alpha}$ are the expansion coefficients of the i^{th} TB single-particle wavefunction $\psi_i(\mathbf{r}) = \sum_{\mathbf{R}\alpha} c^i_{\mathbf{R}\alpha}\phi_{\alpha\mathbf{R}}(\mathbf{r})$, in terms of the atomic orbitals $\phi_{\alpha\mathbf{R}}(\mathbf{r})$ localized at the position $\mathbf{R}$. In Eq. 1 the variation of the Coulomb interaction is taken into account only on a length scale of the order of the lattice vectors but not inside one unit cell. This is well justified due to the long ranged, slowly varying behavior of the Coulomb interaction. For $|\mathbf{R}-\mathbf{R}'| = 0$ the evaluation of the integral in Eq. (2) can be done quasi-analytically by expansion of the Coulomb interaction in terms of spherical harmonics [16]. The details can be found in Ref. [6].

In contrast to the Coulomb matrix elements, the short range contributions dominate the dipole matrix elements. Therefore, it is necessary to connect the calculated TB coefficients directly to the underlying set of atomic orbitals. A commonly used approach is the use of Slater orbitals [17]. These orbitals include the correct symmetry properties of the underlying TB coefficients but lack the essential assumption of orthogonality with respect to different lattice sites, since they have been developed for isolated atoms. We

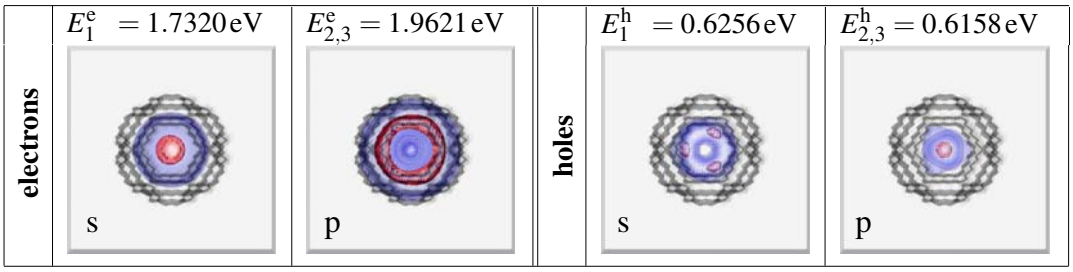

Fig. 1 The structure of the QD is shown from atop. Isosurfaces of the electron and hole charge density, respectively, with 20% (blue) and 80% (red) of the maximum value are depicted. The first two shells for electrons (left) and holes (right) are shown. For the two-fold degenerate p-shell only one state is visualized, as the other one looks alike. The C_{3v}-symmetry of the QD geometry and the underlying wurtzite crystal is most evident for the hole states. The corresponding energies ($E_{1,2,3}^{e,h}$) are measured from the valence band maximum of bulk GaN.

overcome this problem by using numerically orthogonalized Slater orbitals [6]. These orthogonalized orbitals fulfill all basic requirements, regarding the symmetry, locality, and orthogonality of the basis orbitals underlying the TB formulation.

The microscopically evaluated single-particle states and Coulomb interaction matrix elements in the configuration-interaction (CI) calculation are used to determine the multiexciton eigenstates. [3, 4] If one considers only the bound single-particle states for the electrons and holes, the eigenvalue problem for a given number of electrons and holes has a finite dimension. Therefore it can be solved without further approximations and the Coulomb interaction between all the different possible configurations of carriers in the considered bound states is fully taken into account. In order to find the eigenvalues and eigenfunctions of the interacting problem, the many-body Hamiltonian is expressed in terms of the uncorrelated basis and the resulting Hamiltonian matrix is diagonalized. This yields an expansion of the interacting eigenstates of the system for a given number of electrons and holes in terms of the uncorrelated basis states. With these states one can then calculate emission or absorption spectra between the interacting eigenstates of the QD system using Fermi's golden rule.

3 Results

We consider here a small lens-shaped QD with diameter $d = 4.5\,\mathrm{nm}$ and height $h = 1.6\,\mathrm{nm}$. This lens-shaped QD confines three bound electron states. These states are included in the configuration interaction calculation, together with the first three bound hole states which are spectrally well separated from the other hole states. The one-particle states are visualized in Fig. 1. The dominant orbital character for the electron states stems from the single atomic s-orbitals, while for the hole states a strong intermixing of the atomic p-orbitals is observed. Note that the p-shell for the electrons and holes are, apart from the spin degeneracy, both two-fold degenerate. This may appear suprising since it is known that in the case of the InGaAs system the p-shell is split if an atomistic description of the electronic states is employed [18]. In the nitride case, however, the symmetry group of the structure is different and indeed supports an exact degenerate p-shell [19]. We emphasize that the proper treatment of the single particle states, and therefore all optical properties, requires a multiband treatment like $\mathbf{k}\cdot\mathbf{p}$, pseudopotential or a tight-binding approach and cannot be accounted for by single-band effective-mass approaches.

With the inclusion of the internal field the electron states are shifted towards the cap of the QD, while the hole states are constrained to a few atomic layers at the bottom. Obviously this spatial separation of electron and hole wavefunctions leads to reduced dipole matrix elements. Besides the influence on the oscillator strength, the additional confinement of the electrons into the cap of the QD increases the electronic Coulomb matrix elements. The internal electric field shifts the electron single-particle states to

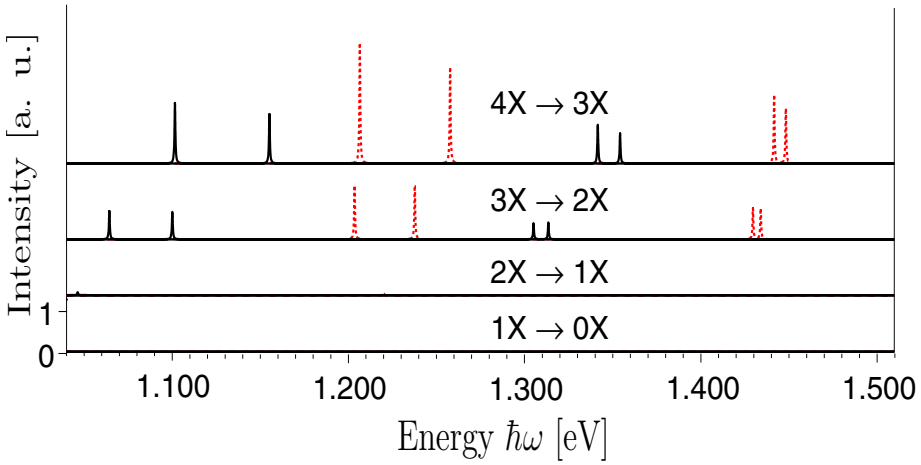

Fig. 2 Emission spectra with (solid-black lines) and without (dashed-red lines) built-in field. The initial states are ground-states for different numbers of excitons with total spin z-component $S_z = 0$.

lower energies, while the hole states are shifted to higher energies. Consequently, the electrostatic built-in field leads to an overall redshift in the single particle energy-gap, that is also known from the quantum-confined Stark effect (QCSE).

With the discussed single-particle states Coulomb and dipole matrix elements are calculated. They enter in our CI calculation as input parameters. This leads to the multi-exciton emission spectra, depicted in Fig. 2 for the investigated QD. The spectra are shown with and without the influence of the built-in field for an initial filling with one up to four excitons. The quantum-confined Stark effect is clearly visible as an overall redshift of the spectra and also manifests itself in a reduction of the oscillator strengths by about a factor of two. For the investigated small lens-shaped InN/GaN QDs, we find vanishing exciton and biexciton ground-state emission [5], due to the underlying C_{3v} symmetry of the system [19]. At higher excitation conditions strong emission from three to four exciton complexes is obtained . Furthermore, with increasing number of electron and hole pairs a strong blueshift can be observed. This feature can already be explained by the strong Hartree contributions that arise as the envelopes for the electrons and holes are quite different. This strong deviation of the envelopes leads to Hartree-Fock terms that would at least partly cancel in the case of identical envelopes. Note that the energetic shift with increasing number of excitons is by far more pronounced in the presence of the internal fields as the stronger separation of the electron and hole wave functions is accompanied by stronger Hartree-fields.

4 Conclusion

An empirical sp^3 TB-model has been applied to the calculation of the electronic states of a self-assembled InN/GaN QD. We have calculated the first three bound electron and hole states, localized in the region of the dot, by numerical diagonalization of the huge TB matrix. The influence of the internal electric field on the single particle states and energies is studied. The built-in field leads to a red shift in the single particle energy-gap of the QD. Inside the electrostatic field, the electron states move towards the top and the hole states move down to the bottom of the QD.

Furthermore, the multiexciton emission spectra are calculated with microscopically determined input parameters, which fully takes into account the underlying wurtzite crystal lattice. The inclusion of the internal electric field results in an overall redshift of the spectra and a decrease of the dipole matix elements, due to the spatial separation of electron and hole wavefunctions. For the small lens-shaped InN/GaN QD investigated here, we find a vanishing exciton and biexciton ground state emission.

Acknowledgements The authors acknowledge financial support by the Deutsche Forschungsgemeinschaft and a grant for CPU time from the John von Neumann Institute for Computing at the Forschungszentrum Jülich.

References

[1] R. Santoprete, B. Koiller, R. B. Capaz, P. Kratzer, Q. K. K. Liu, and M. Scheffler, Phys. Rev. B **68**, 235311 (2003).
[2] S. Schulz and G. Czycholl, Phys. Rev. B **72**, 165317 (2005).
[3] A. Barenco and M. A. Dupertuis, Phys. Rev. B **52**, 2766 (1995).
[4] N. Baer, P. Gartner, and F. Jahnke, Eur. Phys. J. B **42**, 231 (2004).
[5] N. Baer, S. Schulz, S. Schumacher, P. Gartner, G. Czycholl, and F. Jahnke, Appl. Phys. Lett. **87**, 231114 (2005).
[6] S. Schulz, S. Schumacher, and G. Czycholl, Phys. Rev. B **73**, 245327 (2006).
[7] J. C. Slater and G. F. Koster, Phys. Rev. **94**, 1498 (1954).
[8] D. Fritsch, H. Schmidt, and M. Grundmann, Phys. Rev. B **69**, 165204 (2004).
[9] G. L. Zhao, D. Bagayoko, and T. D. Williams, Phys. Rev. B **60**, 1563 (1999).
[10] I. Vurgaftman and J. R. Meyer, J. Appl. Phys. **94**, 3675 (2003).
[11] S. Sapra and D. D. Sarma, Phys. Rev. B **69**, 125304 (2004).
[12] S. De Rinaldis, I. D'Amico, and F. Rossi, Appl. Phys. Lett. **81**, 4236 (2002).
[13] B. Monema, P. P. Paskov, and A. Kasi, Superlattices Microstruct. **38**, 38 (2005).
[14] U. M. E. Christmas, A. D. Andreev, and D. A. Faux, J. Appl. Phys. **98**, 073522 (2005).
[15] L.-W. Wang and A. Zunger, J. Chem. Phys. **100**, 2394 (1994).
[16] I. Schnell, G. Czycholl, and R. C. Albers, Phys. Rev. B **65**, 075103 (2002).
[17] S. Lee, L. Jönsson, J. W. Wilkins, G. W. Bryant, and G. Klimeck, Phys. Rev. B **63**, 195318 (2001).
[18] G. Bester and A. Zunger, Phys. Rev. B **71**, 045318 (2005).
[19] N. Baer, S. Schulz, P. Gartner, S. Schumacher, G. Czycholl, and F. Jahnke (in preparation).

